Micro and Nanoscale Study of Calcium and Rare Earth Element Fluorcarbonates

Establishing a Link Between Mineral Structure and Genesis

Roberto Conconi
Department of Earth and Environmental Sciences, University of Milano-Bicocca, Piazza della Scienza 4, 20126, Milano

DOI: 10.19276/plinius.2025.01.008

INTRODUCTION

The development of green technologies to establish the basis for a low-carbon future is leading to an increase in the demand for critical raw materials (CRMs) (Vidal et al., 2013). Indeed, green and renewable technologies such as wind turbines, electric vehicles and solar panels require a large quantity of CRM, including rare earth elements (REE), platinum group metals (PGMs), Li and Co, among others.

For these reasons and because it is estimated that the demand for REE will constantly grow in the next decades, innovative methods for extracting REE are envisaged. There are over 200 mineral species containing REE, but only a few contain enough REE to have the potential for forming economic ore deposits (Kanazawa & Kamitani, 2006). The primary ore minerals for REE are: REE-carbonates, -fluorcarbonates and -phosphates like bastnäsite, parisite, synchysite, monazite, and xenotime. However, despite the economic importance of REE and their bearing minerals, a lot of unanswered questions about the mechanisms that govern the REE transport and deposition in natural systems, as well as the crystallization of REE-bearing phases, remain. These challenges arise from the difficulty of replicating the complex natural conditions in the laboratory and the inherent challenge of separating different REE. In this regard, it is universally recognized, as well as often forgotten, that fundamental research is the nourishment of applied research. Indeed, mineralogical and crystallographic studies on REE-bearing minerals may shed light on their nature and genesis, eventually suggesting more successful prospection routes, enhanced metallurgical processes and recycling strategies. For these reasons, (Ca-REE) fluorcarbonates (hereafter CRFC) have been identified as the ideal mineral group for conducting mineralogical and crystallographic studies. The interesting characteristic of CRFC is that they form a polysomatic series (Donnay & Donnay, 1953; Conconi et al., 2023, 2025a, b), where bastnäsite and synchysite are the end members, and different intermediate polysomes, such as parisite and röntgenite, have been identified over the years. The study of polysomatism is particularly significant, as the intergrowths of different polysomes may indicate changes in crystallization conditions or fluid composition (Gysi & Williams-Jones, 2015).

In this work, various CRFC samples from different localities and geological settings were studied using multiple techniques such as scanning electron microscopy (SEM) coupled with energy dispersive spectroscopy (EDS) and electron backscattered diffraction (EBSD), Raman spectroscopy, transmission electron microscopy (TEM), precession-assisted three-dimensional electron diffraction (3DED) and single-crystal X-ray diffraction (SCXRD). The goal was to link their micro- and nanostructures to the large-scale processes responsible for their formation. Indeed, micro- and nanoscale observations proved fundamental in fully characterizing these minerals and provided important insights into the possible crystallization mechanisms of CRFC. These findings aim to contribute valuable knowledge to the understanding of the complex processes behind the crystallization of these minerals.

SAMPLES

The samples studied in this work come from two different localities: Mount Malosa (Malawi, Africa) and Cuasso al Monte (Varese, Italy). The CRFC from Mount Malosa were previously described by Guastoni et al. (2009, 2010) and Capitani (2019). They are polycrystals made of stacking different CRFC (Fig. 1a). They typically exhibit a yellowish-reddish colour and are associated with aegirine. In contrast, the CRFCs from Cuasso al Monte occur in three distinct morphologies, all of which are micrometer-sized: rosette-like aggregates, hexagonal prisms, and blocky subhedral shape (Fig. 1b, c, d).

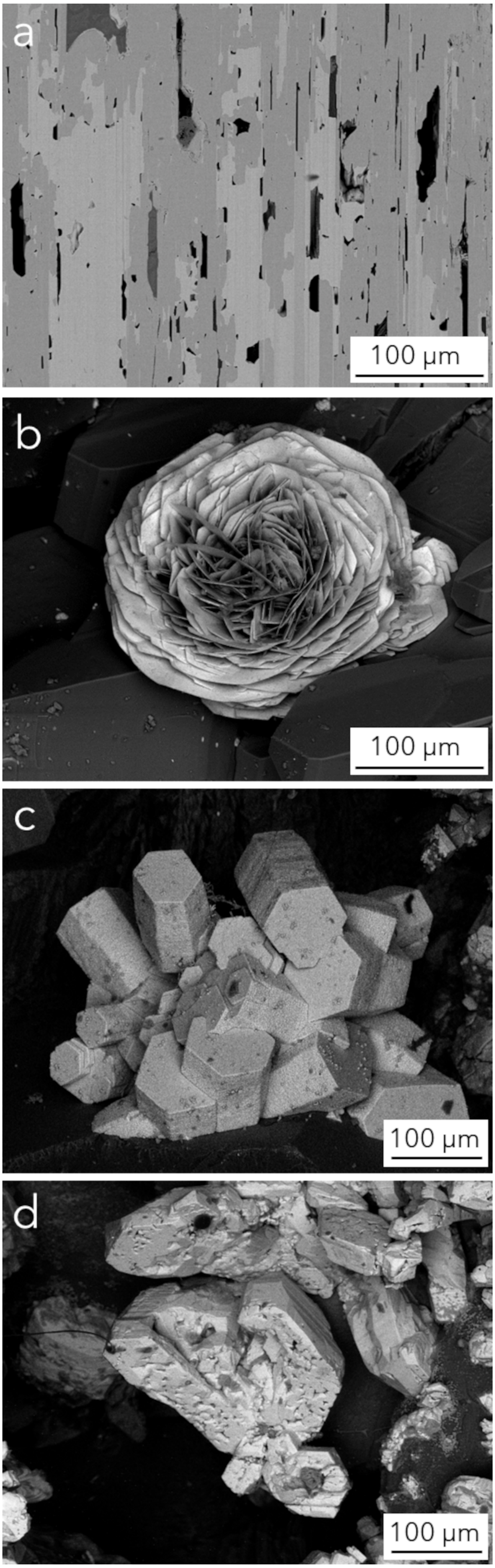

Figure 1 SEM images showing: ***a)*** *CRFC from Mount Malosa showing syntactic intergrowths.* ***b, c, d)*** *CRFCs from Cuasso al Monte displaying three different morphologies (Conconi et al., 2023; 2025a).*

A MULTI-METHODOLOGICAL IDENTIFICATION OF CRFC

The CRFCs from Mount Malosa were studied using a multimethodological approach to provide a roadmap for the correct identification of these minerals. First, the samples were analysed using SEM-EDS to gain an initial understanding of their microstructure and chemical variability at a microscopic scale. As expected, the samples display the parallel banding typical of CRFC syntactic intergrowths (Fig. 1a). EDS spot analyses revealed the presence of different CRFC polysomes such as bastnäsite, parisite, röntgenite, synchysite, and several unnamed intermediate terms.

Subsequently, EBSD analyses were conducted to: (1) establish the initial orientation of the samples; and (2) evaluate the method's capability to distinguish different polysomes. EBSD successfully established sample orientation, but it failed to discriminate between the various polysomes. This limitation can be understood considering that electron diffraction is dominated by heavy atoms, and in CRFC the stacking of heavy atoms (Ca and REE) is hexagonal for all the terms of the series.

Raman spectroscopy was performed on samples with different crystal orientations. Generally, different polysomes can be identified by analysing the $v_1(CO_3)$ symmetric stretching vibration of the carbonate group. Bastnäsite shows a single band; synchysite displays two bands; and the intermediate terms exhibit three bands, with intensity ratios that vary depending on orientation (Fig. 2a).

TEM observations revealed nanoscale disorder characterized by intergrowths of different stacking faults. At the TEM scale, the Mount Malosa samples appear to consist mostly of bastnäsite–parisite intergrowths, with minor areas containing more ordered polysomes (Fig. 2b, c).

This suggests that while SEM and Raman spectroscopy provide an overview of the sample composition, TEM remains the most effective technique for the detailed characterization of CRFCs.

These observations indicate that the most common microstructure in Mount Malosa CRFCs consists of rhythmic parisite–bastnäsite intergrowths, along with several more or less ordered intermediate polysomes. The observed microstructure supports a primary growth mechanism in which fluorcarbonates crystallize from a fluid near thermodynamic equilibrium, with conditions rapidly and repeatedly crossing the parisite–bastnäsite stability boundary, rather than following a stepwise progression toward equilibrium (for more details, see Conconi et al., 2023).

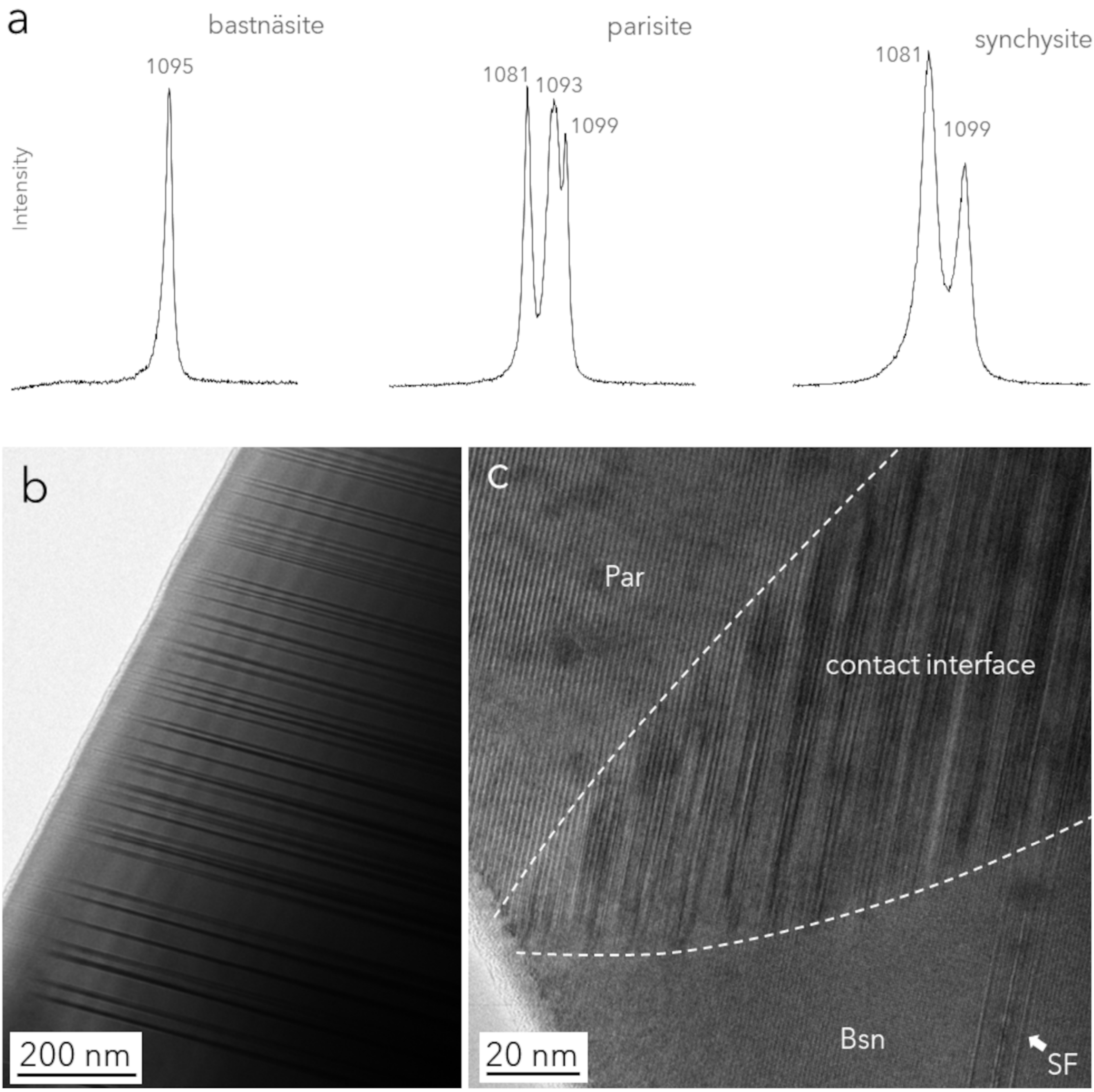

Figure 2 a) *Raman spectra of bastnäsite, parisite and synchysite, showing the different numbers of bands associated with the* $\nu_1(CO_3)$ *symmetric stretching vibration of the carbonate group.* ***b)*** *TEM image showing the typical nanostructures of CRFC from Mount Malosa, made of dense stacking faults.* ***c)*** *Contact interface between parisite (Par) and bastnäsite (Bsn); stacking faults (SF) are visible within the bastnäsite.*

A VARIETY OF MORPHOLOGIES, COMPOSITIONS AND NANO-STRUCTURES: INSIGHTS INTO REE PARTITIONING AND MOBILITY

At Cuasso al Monte, CRFCs exhibit a wide variety of morphologies and compositions. Three main types have been identified: *i)* synchysite-(Ce) occurring as hexagonal prisms (Fig. 1c) and rosette-like aggregates (Fig. 1a); *ii)* bastnäsite-(Ce) forming blocky aggregates (Fig. 1d); and *iii)* bastnäsite-(Nd) forming desert rose-like intergrowths (Fig. 3e). Among these, hexagonal prism synchysite-(Ce), rosette-like synchysite-(Ce), and desert rose-like bastnäsite-(Nd) have been studied in greater detail.

The hexagonal prisms synchysite-(Ce) show a core-rim chemical zoning with three different areas: *i)* a core enriched in Ce, La and Nd; *ii)* a rim enriched in Y and *iii)* an outer rim enriched in Th (Fig. 3a). TEM analysis reveals the presence of hematite nanocrystal inclusions (Fig. 3b), while selected area electron diffraction (SAED) patterns show a superstructural order in synchysite with a periodicity of approximately 93 Å, a value that is commensurate with the quarter-cell of synchysite (~4.6 Å), moreover its structure has been refined using both SCXRD and 3DED. This superstructure suggests that the hexagonal prism synchysite-(Ce) may represent a long-range polytype, which likely lacks a distinct thermodynamic stability field and may have formed via a screw dislocation

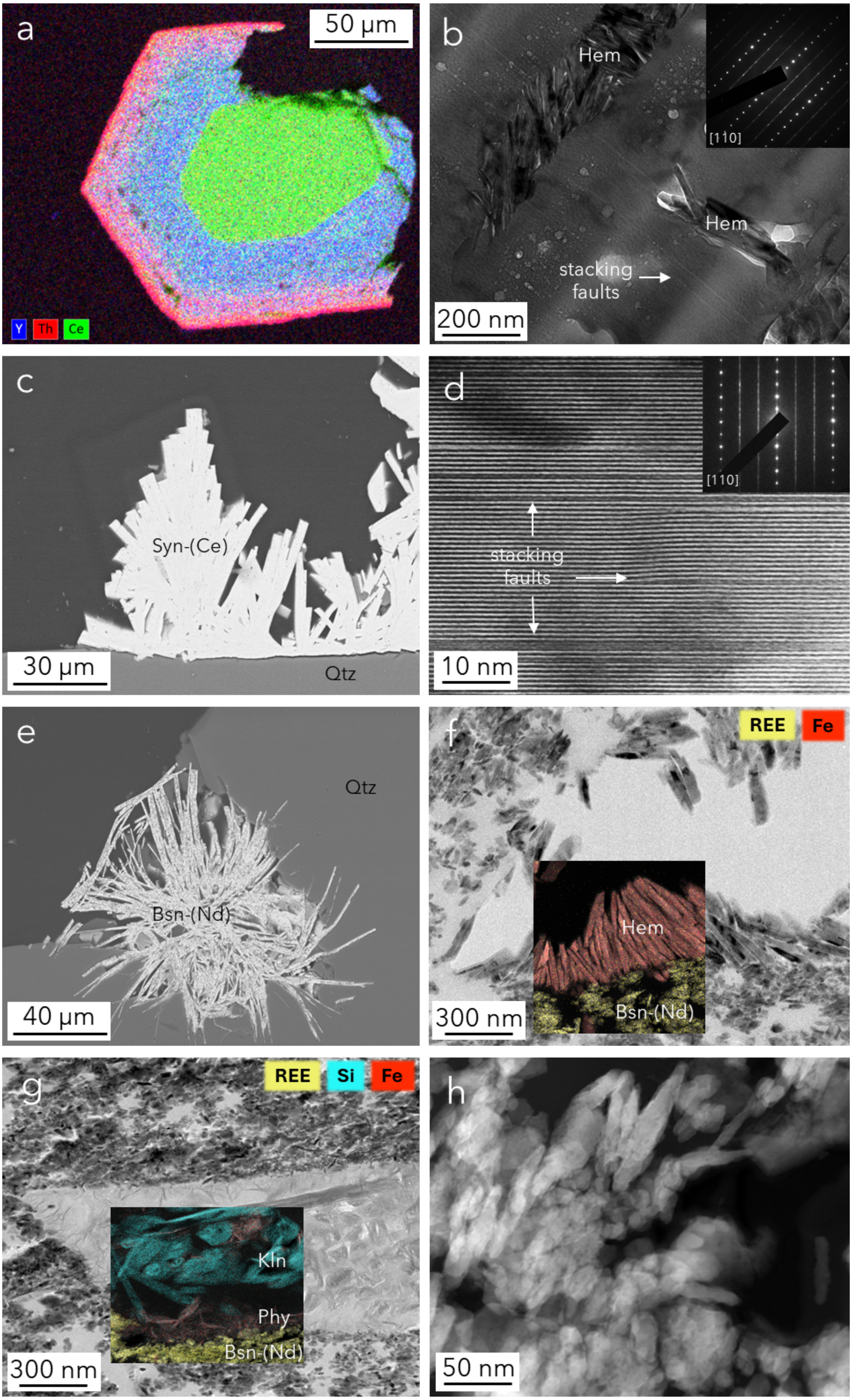

Figure 3 ***a)*** *SEM-EDS map of the hexagonal prism synchysite-(Ce) showing the chemical zoning.* ***b)*** *TEM image and corresponding SAED pattern of the hexagonal prism synchysite-(Ce), showing the presence of hematite nanocrystals and stacking faults within the crystal.* ***c)*** *SEM image showing the rosette-like synchysite-(Ce).* ***d)*** *High resolution TEM image and corresponding SAED pattern of* ***(c)*** *showing the presence of stacking faults.* ***e)*** *SEM image showing the desert rose-like bastnäsite-(Nd).* ***f, g)*** *TEM images showing the intergrowth of bastnäsite-(Nd) with hematite (Hem), phyllosilicates (Phy) and a kaolinite-like phase (Kln).* ***h)*** *TEM image showing the rod shape morphology of bastnäsite-(Nd) nanocrystals, (images taken and modified from Conconi et al., 2025a, b).*

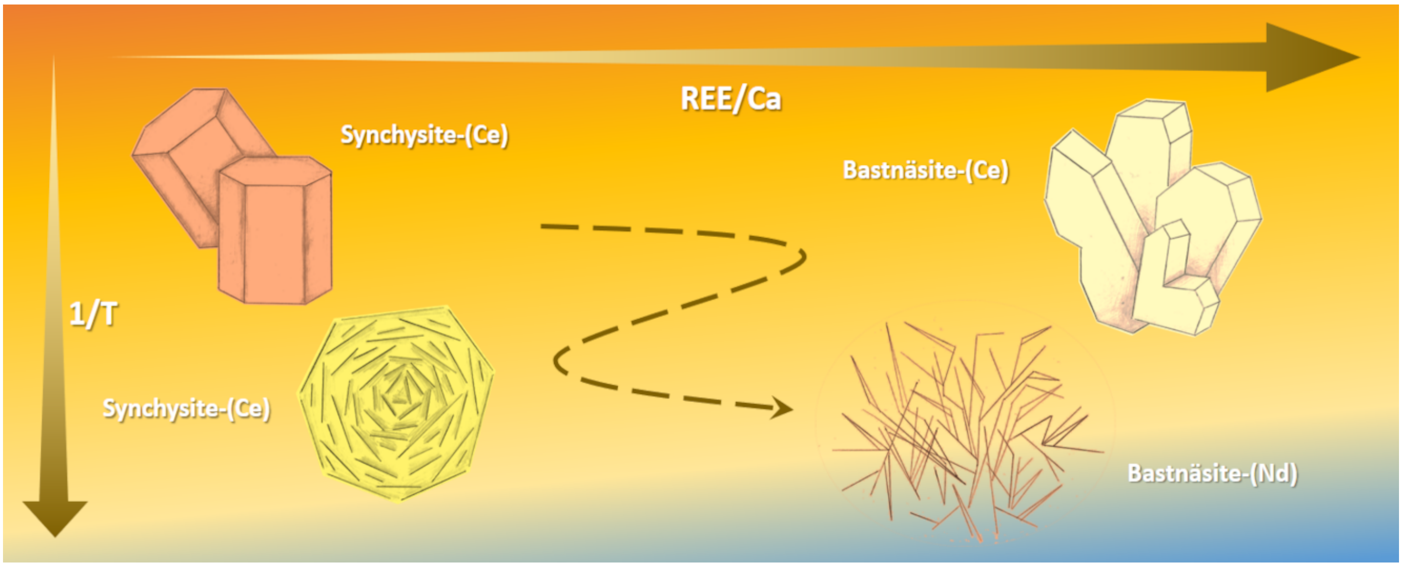

Figure 4 *Schematic drawing of the possible crystallization pathway for the CRFCs of Cuasso al Monte (Conconi et al., 2025a).*

growth mechanism. However, this mechanism appears incompatible with the sharp core–rim chemical zoning. It is therefore plausible that the core initially formed via screw dislocation, followed by a second stage of growth on the crystal's outer faces from a Y-enriched liquid. The outermost rim, enriched in Th, likely formed through diffusive exchange or REE substitution by Th (Conconi et al., 2025b).

Rosette-like synchysite-(Ce) forms thick, flat, and compact lamellae (Fig. 3c). TEM-EDS analysis reveals that these lamellae have a nanostructure in which the rosette-like "petals" are single crystals, with their shortest dimension oriented parallel to **c***, the stacking direction of Ca, CeF, and (CO_3) layers. Each petal can thus be interpreted as a stubby prism. SAED patterns and lattice fringe images indicate the presence of polysomatic and polytypic disorder, reflecting structural complexity at the nanoscale (Fig. 3d).

In contrast, desert rose-like bastnäsite-(Nd) forms thinner and slightly bent lamellae with a widespread porosity (Fig. 3e). At the nanoscale, bastnäsite-(Nd) shows a complex nanostructure recalling the gypsum or calcite "desert rose" (although at a smaller scale), made of an intergrowth of bastnäsite and hematite nanocrystals, with also phyllosilicates, including a kaolinite-like phase (Fig. 3f, g). The CRFC nanocrystals generally appear as nanorods less than 50 nm in length (Fig. 3h). Hematite was observed both as nanorods up to 200 nm in length and as irregular nanoparticles, generally dispersed within bastnäsite, but sometimes forming clusters. Phyllosilicates are present either along the rim of the rosette-like "petals" or within interstices left by bastnäsite-hematite intergrowths. Overall, lattice fringe images and the SAED patterns of the bastnäsite-(Nd) show an ordered structure. Furthermore, a distinctive feature of this phase is the REE distribution, with Nd as the dominant REE, followed by La and Ce.

At Cuasso al Monte, the CRFC were among the latest phases to crystallize from a F-rich hydrothermal fluid (Capitani et al., 2018). Based on our observations, a possible crystallization pathway for CRFCs has been proposed (Fig. 4): *i)* synchysite-(Ce) prisms formed early in the crystallization sequence from a Ca- and F-rich fluid, at relatively low cooling rate; *ii)* the Ca-depleted fluid then reached the condition to form blocky bastnäsite-(Ce), still at relatively low cooling rates; *iii)* the fluid reached again, at slightly lower temperatures, supersaturation conditions for Ca and Ce, crystallizing rosette-like synchysite-(Ce). Indeed, so many "petals" of synchysite-(Ce) may represent fast nucleation events under a relatively high cooling rate that resulted into undeveloped prisms; *iv)* the remaining fluid, at that point depleted in Ca and Ce and at low temperature, crystallized rosette-like bastnäsite-(Nd) (Conconi et al., 2025a).

CONCLUSIONS

In the present study, CRFCs belonging to the bastnäsite-synchysite series were investigated to establish a relationship between their micro- and nano-structure and the genetic mechanisms driving their crystallization. A multimethodological approach was employed, using various analytical techniques, including SEM-EDS, EBSD, Raman spectroscopy, TEM-EDS, 3DED, and SCXRD. Initially, a roadmap for identifying CRFC polysomes was developed. The results demonstrate that Raman spectroscopy effectively distinguishes CRFC members based on the symmetric $v_1(CO_3)$ stretching vibration of the carbonate group. Although Raman spectroscopy can effectively determine the Ca/(Ca+REE) ratio in CRFC, it may not be suitable for distinguishing between ordered and disordered intergrowths with similar composition. For this reason, TEM-EDS remains the ultimate technique for polysome identification. However, TEM also has its own intricacies. Since most high-resolution TEMs have a limited tilt range, the sample needs to be pre-oriented before preparation; for this purpose, EBSD can be very useful. Indeed, EBSD can easily distinguish CRFC among other phases and correctly provides their orientation relationship, but under routine application, it fails to distinguish among different polysomes.

The micro- and nano-scale analysis revealed diverse structures among the CRFC samples, which can provide insights into the mechanisms responsible for their crystallization. In Mount Malosa CRFCs, the most common microstructure is rhythmic parisite-bastnäsite intergrowths alongside a number of more or less ordered intermediate polysomes. The observed microstructure indicates a primary growth mechanism where CRFCs crystallized from a fluid near thermodynamic equilibrium, with conditions repeatedly crossing the parisite–bastnäsite stability boundary.

In contrast, CRFCs from Cuasso al Monte exhibit a wider variety of morphologies, compositions, and nanostructures. From these observations, it was possible to infer a crystallization pathway involving an initial F-rich fluid that, upon cooling, sequentially precipitated different CRFC phases under evolving physicochemical conditions.

In conclusion, this study highlights that advancements in imaging and analytical techniques have enabled the acquisition of chemical and structural information with exceptional spatial resolution, which is crucial for fully characterizing the material under analysis. Indeed, information obtained from the micro- to the nano-scale has proven important in explaining macro-scale processes, such as crystallization and elements partitioning. Understanding these processes is of paramount importance, especially considering that CRFC are the primary ore for REE.

REFERENCES

Capitani, G. (2019) - HRTEM investigation of bastnäsite–parisite intergrowths from Mount Malosa (Malawi): ordered sequences, polysomatic faults, polytypic disorder, and a new parisite-(Ce) polymorph. Eur. J. Mineral., 31, 429–442.

Capitani, G., Mugnaioli, E., Gentile, P. (2018) - Submicrometer yttrian zircon coating and arborescent aeschynite microcrystals on truncated bipyramidal anatase: An electron microscopy study of miarolitic cavities in the Cuasso al Monte granophyre (Varese, Italy). Am. Mineral., 103, 480–488.

Conconi, R., Fumagalli, P., Capitani, G. (2023) - A multimethodological study of the bastnäsite-synchysite polysomatic series: Tips and tricks of polysome identification and the origin of syntactic intergrowths. Am. Mineral., 108, 1658–1668.

Conconi, R., Gentile, P., Fumagalli, P., Nieto, F., Capitani, G. (2025a) - CaREE-fluorcarbonates: A variety of morphologies, compositions and nanostructures with insights into REE partitioning and mobility. Lithos, 108033, 504–505.

Conconi, R., Merlini, M., Fumagalli, P., Mugnaioli, E., Folco, L., Capitani, G. (2025b) - Average Structure and Microstructure of Synchysite-(Ce) from Cuasso al Monte (Varese, Italy). Eur. J. Mineral., 37, 233–247.

Donnay, G. & Donnay, J.D.H. (1953) - The crystallography of bastnäsite, parisite, röntgenite and synchysite. Am. Mineral., 38, 932–963.

Guastoni, A., Nestola, F., Giaretta, A. (2009) - Mineral chemistry and alteration of rare earth element (REE) carbonates from alkaline pegmatites of Mount Malosa, Malawi. Am. Mineral., 94, 1216–1222.

Guastoni, A., Kondo, D., Nestola, F. (2010) - Bastnäsite-(Ce) and Parisite-(Ce) From Mt. Malosa, Malawi. Gems Gemol., 46, 42–47.

Gysi, A.P. & Williams-Jones, A.E. (2015) - The thermodynamic properties of bastnäsite-(Ce) and parisite-(Ce). Chem. Geol., 392, 87–101.

Kanazawa, Y. & Kamitani, M. (2006) - Rare earth minerals and resources in the world. J. Alloys Compd., 408–412, 1339-1343.

Vidal, O., Goffé, B., Arndt, N. (2013) - Metals for a low-carbon society. Nat. Geosci., 6, 894–896.